The effect of shaping on RFP dynamics

R. Chahine[1], J. Morales[2], K. Schneider[3] and W.J.T Bos[1]

[1]LMFA, CNRS, Ecole Centrale de Lyon, Université de Lyon, Ecully, France
[2]SPC, EPFL, Switzerland
[3]Institut de Mathématiques de Marseille, Aix-Marseille Université, Marseille, France

Corresponding Author: rchahine@ec-lyon.fr, wouter.bos@ec-lyon.fr

Abstract:

The influence of the shape of the plasma on the dynamics of RFPs is investigated in numerical simulations of fully nonlinear visco-resistive magnetohydrodynamics. The axial mode-spectrum is qualitatively changed in cylinders with elliptic cross-section, and the radial turbulent diffusion is affected. **Even though from the present study it cannot be concluded what the optimal shape of an RFP should be, it is clear that the shape of the cross-section is an important parameter that should be taken into account when optimizing the confinement quality of an RFP.**

1 Introduction

Tokamaks and Reversed Field Pinches (RFPs) are toroidal fusion plasmas with a similar magnetic geometry. In both types of plasma the combination of an imposed toroidal magnetic field combined with a poloidal magnetic field, associated with an induced toroidal current, result in a helical field, around the toroidal axis. The difference between the plasmas is the strength of the toroidal magnetic field, which needs to be much larger than the poloidal field in tokamaks, whereas it is of the same order of magnitude in RFPs. This requirement is due to the dangerous MHD instabilities, or disruptions, in tokamaks [1], which lead to loss of confinement.

The RFP works in this unstable regime, but takes advantage of the nonlinear saturation of the instability, thereby bypassing the risk of disruptions and avoiding the need of a very strong (and costly) toroidal magnetic field. Whereas in early research on the RFP the unstable character was seen as a drawback for fusion, it has become increasingly clear that the self-organization of the RFP is actually an asset to reach self-sustained fusion. Indeed in the 2000s, quasi-single-helicity (QSH) states were detected within turbulent flows in the RFX experiment [2–4]. These states are characterized by the appearance of a quiescent helical structure in the plasma core, which improves the plasma confinement [5–7]. Later studies showed that the persistence of these QSH states and the appearance of a Single-Helical Axis at high current regimes [8] can be increased by applying helical magnetic perturbations [9, 10]. These results motivated (a small part of) the fusion community to reconsider the RFP as a suitable candidate for nuclear fusion [11].

Indeed, applying helical magnetic perturbations seems a promising way to affect the self-organized state in an RFP [12]. Another obvious way would be to change directly the shape of the plasma. The optimization of the confinement quality for toroidal fusion plasmas by changing the plasma shape has been the subject of many studies, in particular for tokamaks. For instance, it has been shown that shaping has a beneficial effect on the β limits of tokamaks [13], and increases the total plasma current I in the case of elliptic cross-sections, yielding thus a better confinement.

Investigations on the influence of shaping on the confinement properties of RFPs are, however, relatively scarce. Some rare examples of experimental observations were presented in [14,15], and numerical investigations are reported in references [16,17] where two-dimensional equilibrium studies were carried

out in order to investigate the shaping effect on RFP plasmas. Their work led to the conclusion that shaping does not bring an advantage to the plasma dynamics in RFPs and is even destabilizing in the case in which the poloidal cross-section is elongated. These studies focused on the stability properties of RFPs, but did not consider the fully developed nonlinear dynamics. Here we proceed one step further in the investigation of the effect of changing the shape of the cross-section of RFPs by considering the fully nonlinear dynamics within a resistive fluid description. More precisely, we investigate the effect of elongation of the poloidal cross-section on plasmas in RFPs by means of direct numerical simulations using a three-dimensional MHD pseudo-spectral solver [18]. We consider the simplified case where the torus is modeled by a straight periodic cylinder. **We justify the choice of this simplification as follows. In reference [19], we compared the straight-cylinder approach to fully toroidal simulations. We showed that most of the qualitative features remained unchanged. The most significant change was the appearance of a toroidally invariant mode, the influence of which we do therefore necessarily neglect in the present work. It is true that considering the effect of curvature on the dynamics of RFP could be interesting, but we aim at the understanding of the two effects (curvature and shape of the cross-section) independently in order to pinpoint the most important physical effects, before considering their possible interplay. Furthermore, in Paccagnella et al. [16] the influence of curvature was considered with respect to the stability properties of RFPs and its effect was shown to be minor.**

In the present work is shown that elongation of the cross-section has a significant effect on the dynamics of the plasma. **To probe the confinement, we consider the advection of a passive scalar, injected in the core of the plasma. The mean scalar profile that establishes allows us to directly determine the turbulent diffusivity associated with the RFP dynamics. The results of our simulations show that** in some cases the confinement compared to circular RFPs is improved by shaping.

The remainder of the manuscript is organized as follows. Section 2 presents the governing equations, recalls briefly the numerics and the relevant physical parameters. Results are shown in section 3 and section 4 discusses the choice of the length scales. Conclusions are drawn in section 5.

2 Equations, numerical methods and parameters

2.1 Visco-resistive MHD equations

In the present work, we consider a plasma characterized by constant, and uniform permeability μ, permittivity ϵ and conductivity σ. **The more complicated case of non-uniform conductivity was considered in reference [20].** In the magnetohydrodynamic (MHD) description that we consider, the governing equations are the incompressible Navier-Stokes equations including the Lorentz force, and the induction equation. Normalizing these quantities by the Alfvén velocity $C_A = B_0/\sqrt{\rho\mu}$, a reference magnetic field B_0 and a conveniently chosen length scale $\mathcal{L}$ leads to the following expressions,

$$\frac{\partial \boldsymbol{u}}{\partial t} + \boldsymbol{u} \cdot \nabla \boldsymbol{u} = -\nabla P + \boldsymbol{j} \times \boldsymbol{B} + \frac{P_m}{S}\nabla^2 \boldsymbol{u}, \tag{1}$$

and

$$\frac{\partial \boldsymbol{B}}{\partial t} = \nabla \times (\boldsymbol{u} \times \boldsymbol{B}) + S\nabla^2 \boldsymbol{B}, \tag{2}$$

where the magnetic Prandtl number $P_m = \nu/\lambda$ is the ratio of kinematic viscosity over magnetic diffusivity, $S = B_0\mathcal{L}/\lambda$ the Lundquist number and $\rho = 1$ the density. The current density is given by

$$\boldsymbol{j} = \boldsymbol{\nabla} \times \boldsymbol{B}. \tag{3}$$

The velocity field $\boldsymbol{u}$ and the magnetic field $\boldsymbol{B}$ are both divergence free,

$$\boldsymbol{\nabla} \cdot \boldsymbol{u} = 0, \tag{4}$$

$$\boldsymbol{\nabla} \cdot \boldsymbol{B} = 0. \tag{5}$$

3

The incompressibility condition (4) allows to obtain the pressure from the velocity field by taking the divergence of the momentum equation (1) and solving the resulting Poisson-equation. We think it is important to retain this feature in the dynamics unlike in previous investigations of RFPs (e.g. [21, 22]), where the pressure was entirely neglected invoking low-β dynamics. We thus take into account the influence of pressure on the dynamics, but we neglect all compressibility effects and consider the dynamics of an isothermal plasma. Note that imposing incompressibility was shown to diminish the reversal of the magnetic field [23], and this will thus necessarily be the case in the present investigation. We note here that the resistivity profile can also influence the reversal [24]. The combined influence of shaping, compressibility and non-uniform resistivity constitutes an interesting perspective for future work.

Initially, in the plasma a uniform current density j_0 in the z-direction and an axial magnetic field B_{z0} are imposed, resulting in a helically shaped magnetic field. The current density j_0 will induce an elliptical magnetic field B_{p0} parallel to the elliptic boundaries. At later times the magnetic field will reorganize through an interplay with the velocity field, and the total magnetic field will then consist of B_{z0} and B_{p0} plus the self-induced contributions. At the boundaries the velocity is imposed to be zero and the magnetic field is parallel to the boundaries. The value of the poloidal parallel magnetic field at the boundary is fixed and its value is determined by j_0. The expression of B_{p0} in cylindrical coordinates reads,

$$B_r = -\frac{1}{2}j_0 rc\sin(2\theta) \tag{6}$$

$$B_\theta = \frac{1}{2}j_0 r(1 - c\cos(2\theta)) \tag{7}$$

with c the ellipticity which can be expressed as a function of the ellipse's major semi-axis a and minor semi-axis b, i.e,

$$c = \frac{a^2 - b^2}{a^2 + b^2}. \tag{8}$$

Note that the coordinates we use are cylindrical and not elliptical coordinates so that only in the case of the circle the radial vector e_r is everywhere perpendicular to the boundary.
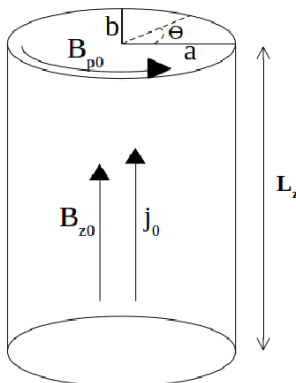

FIG. 1: Sketch of the cylindrical geometry and imposed magnetic field and current density.

The confinement is evaluated by simulating the advection-diffusion equation of a passive scalar T. We thereto solve the following equation simultanuously with equations (1) and (2),

$$\frac{\partial T}{\partial t} + \boldsymbol{u} \cdot \nabla T = \alpha \nabla^2 T + f_T, \tag{9}$$

where α is the scalar diffusivity, chosen equal $\alpha = 10\lambda$, and f_T is a constant source term of value unity, which injects the scalar at a constant rate in a cylindrical region of radius 0.1, in the center of the plasma.

The value at the wall is kept constant and is fixed at zero value, so that the value of T at the center of the plasma is a direct measure of the confinement quality. **In the present work T is therefore an auxiliary quantity, which in the case of small temperature fluctuations, assuming isotropic transport coefficients, could be associated with the temperature. However, in the present case we do not model the interaction of the plasma in the presence of temperature differences, but we consider the case of an isothermal plasma, where T is a passive scalar, advected by the RFP velocity field. An investigation of the fully coupled problem between velocity and temperature will be done in a future work.**

2.2 Numerical methods

Equations (1),(2) and (9) are solved using a pseudo-spectral method in a periodic domain of size $\pi \times \pi \times 8\pi$ with $64 \times 64 \times 512$ grid points. **The aspect ratio of the physical domain containing the plasma is $L_z/2\pi b = 4$.** Spatial derivatives are evaluated in Fourier space and multiplications are computed in physical space. To avoid aliasing errors, i.e., the production of small scales due to nonlinear terms which are not resolved on the grid, the velocity and magnetic fields are dealiased at each time step by truncating its Fourier coefficients using the 2/3 rule [25]. Using the incompressibility condition of the fluid, the pressure term can be eliminated by solving a Poisson equation. A semi-implicit third order time-advancing scheme of Adams-Bashforth type is used to solve the equations, with exact integration of the dissipative and magnetic diffusion terms. Boundary conditions are imposed using a volume penalization method in order to build the cylindrical domain. Detailed description and validation of the method can be found in [26], and an application of the method to investigate RFPs in toroidal domains is reported in previous work [19, 20]. The implementation of the Dirichlet boundary condition for the scalar field is identical to that of the velocity.

To obtain the results presented in section 4 and 5, the equations are integrated for $10^4\tau_A$ Alfvén times, with $\tau_A = \mathcal{L}/C_A$. The results presented in the following are evaluated during the statistically stationary state.

2.3 Shaping parameters

In the present investigation we focus on the influence of the shape of the cross-section on the confinement properties of the plasma. The parameters should be carefully chosen to disentangle the effect of changing the geometry from the effect of changing other control parameters. Considering a periodic cylinder instead of a torus is motivated by this attempt to reduce the number of control parameters to a strict minimum. Even in this simplified geometry, the way in which the parameters are varied is not unique. For instance, if the same toroidal current-density J_z is chosen for two geometries, the mean current I_z will be the same, only if the surface A of the cross-section is kept constant, a condition which we will impose. This will also lead to equal values of the toroidal magnetic flux $\psi = B_z A$, for a given imposed toroidal magnetic field B_z.

The poloidal magnetic B_p field is computed from the current density. Its reference value is evaluated as an average over the circular, or elliptic boundary. Necessarily, keeping the surface A, J_z and B_z fixed, the average value $\overline{B}_p$ varies when changing the shape of the cross-section (the bar indicates a boundary average). The pinch-ratio, defined as

$$\Theta = \frac{\overline{B_p}}{\langle B_z \rangle},\tag{10}$$

where the brackets denote a volume average, therefore depends on the value of the ellipticity c. An important parameter in non-ideal MHD is the Lundquist number, which we define as

$$S = \frac{2\bar{B}_p b}{\lambda},\tag{11}$$

where we used the poloidal magnetic field strength and minor radius as reference quantities. We have chosen b, rather than a, since it is this smallest minor radius which will probably determine the confinement quality. This choice is further discussed in section 4. Imposing the same value of S for different
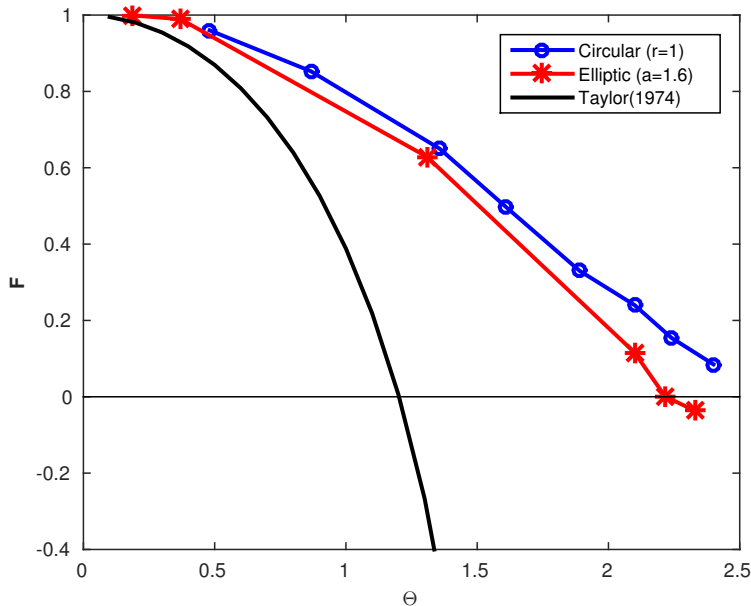
FIG. 2: Field reversal parameter F as a function of the pinch parameter Θ for cylinders with circular and elliptic cross-section. Also shown is Taylor's prediction [27] for reference.

values of the ellipticity allows to determine the value of λ. In all our simulations the value of the magnetic Prandtl number, P_m is chosen unity.

3 Results

3.1 F-Θ stability

The imposed magnetic field in RFPs is unstable for large values of Θ and S, and it will form a dynamic helical structure with a certain amount of chaotic or turbulent motion superimposed.

The modification of the magnetic field can be quantified by the field reversal parameter F, representing the normalized toroidal field at the boundary,

$$F = \frac{\overline{B_z}}{\langle B_z \rangle}. \tag{12}$$

As the current increases, the kink instability increases, leading to the decrease of the toroidal magnetic field at the boundary, so that F decreases as a function of Θ.

This behavior is qualitatively predicted by Taylor's theory [27] and more sophisticated theories allow to improve this agreement [28–30]. In studies [16, 17] based on two-dimensional equilibrium equations, it was shown that shaping does not alter the F-Θ curve. Preliminary simulations for cylinders of small aspect ratio $L_z/2\pi b \sim 2$ and $S \sim 4200$ are carried out and compared with Taylor's prediction [27] for an ellipticity $a = 1.6$. Figure 2 shows the results of the field reversal parameter F versus Θ, which are in reasonable agreement with the two previous studies [16, 17]. **In these references it was shown that shaping had a small destabilizing effect for large curvature, but the $F - \Theta$ curve was unaffected.** Indeed, the two geometries yield roughly the same behavior. However, the reversal parameter is a global parameter and does not give insight into the fine structure of the dynamics. It is this fine structure, constituted by the nonlinear interplay of a large number of modes which will determine
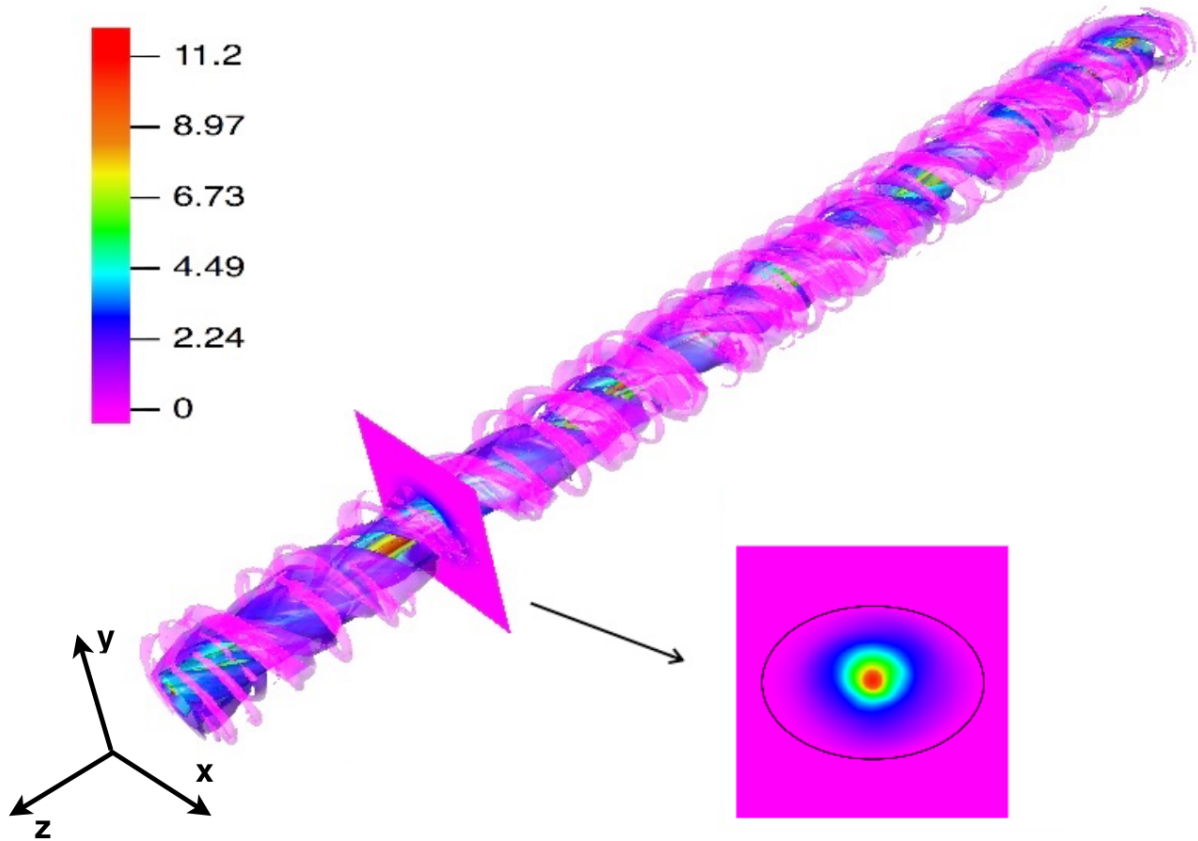
FIG. 3: *Isosurface of axial velocity $u_z = 8.10^{-2}C_A$ colored by the scalar field for an ellipse with $a = 1.2$.*

the confinement quality of a reactor. The modification of the fine structure is now assessed by evaluating the modal behavior of the flow.

3.2   Helical modes and safety factor

We study now the effect of shaping on the helical modes. We have hereto performed simulations for a higher value of S and a larger aspect ratio $L_z/2\pi b = 4$ to approach more realistic conditions. We consider three shapes: a circle with radius $r = 1$, an ellipse with $a = 1.2$ $b = 0.83$ and an ellipse with $a = 1.4$ and $b = 0.714$. The Lundquist number for the three cases is $S \approx 2.10^4$ and the magnetic Prandtl number is $P_m = 1$. To give an idea of the intricate structure of the velocity field, we show in figure 3 an illustration of an instantaneous velocity field. The complex helical structure is clearly visible in this visualisation.

Figure 4 shows the predominance of a magnetic mode with toroidal modenumber $n = 7$ in the circular case, which is consistent with what has been observed in the RFX-mod device. In the elliptical case ($a = 1.2$) a tendency for mode $n = 14$ to dominate is observed, while the magnetic modes $n = 3$ and $n = 4$ contain most of the magnetic energy for $a = 1.4$. This last case seems to be closer to a multiple-helicity state, where not a single mode contains most of the energy. Similar spectral differences are observed in the kinetic spectra, where $n = 0$ and $n = 1$ are the dominating kinetic modes in the circular case, $n = 14$ in the $a = 1.2$ elliptical case, and $n = 8$ in the $a = 1.4$ elliptical case.

The relative influence of the plasma pressure p, compared to the magnetic pressure B^2 is characterized by $\beta \equiv \langle 2p \rangle / \langle B^2 \rangle$, where the brackets denote a volume average. In
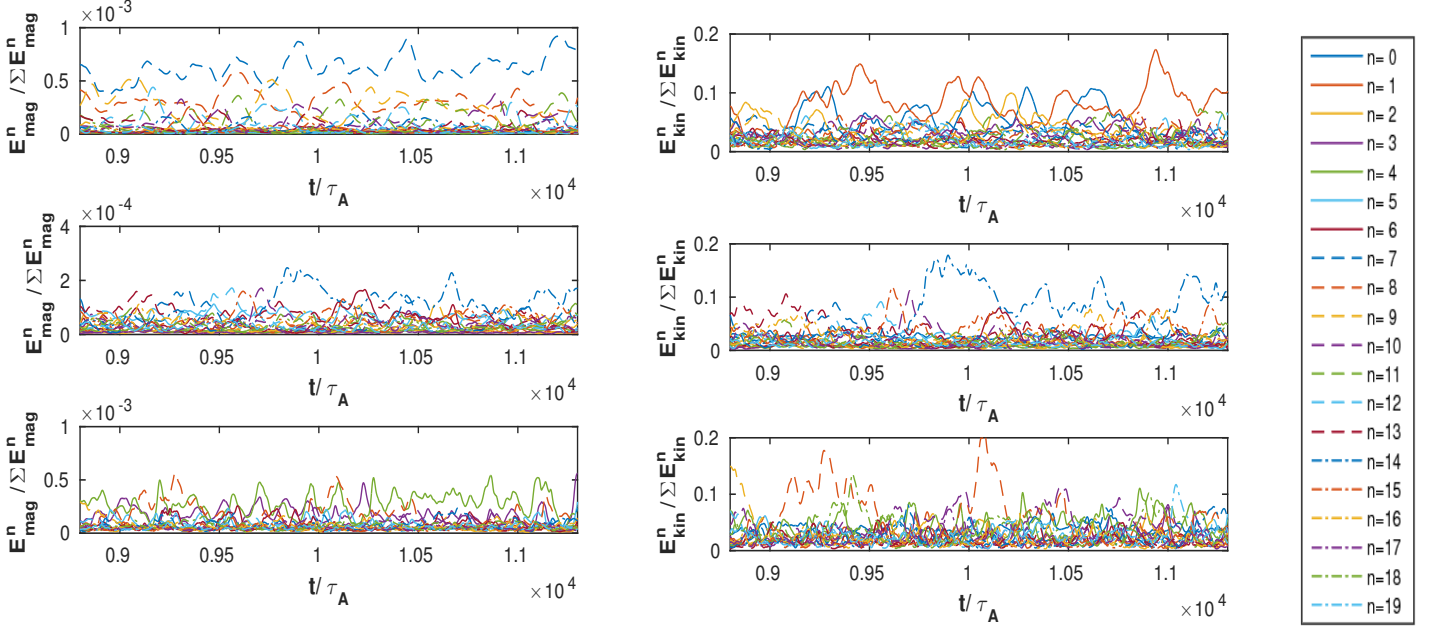
FIG. 4: Axial spectra of magnetic (left) and kinetic (right) energy, normalized respectively by the total magnetic and kinetic energy, considering three shapes, respectively from top to bottom, a circle with radius r=1, an ellipse with major semi-axis a=1.2 and one with a=1.4.

our simulations, the values of β for the geometries with $a = 1; 1.2; 1.4$, are $\beta = 0.29; 0.17; 0.11$, respectively. Further information of the magnetic structure of the plasma is given in Figure 5(a-c), where we display contours of the magnetic flux surfaces in a given cross-section. A clear difference is observed. In the circular case, concentric circular contours are observed, whereas in the $a = 1.2$ case a separatrix appears at the edges of the ellipse. In the most elongated case, the central flux surfaces are destroyed and magnetic islands appear.

The safety factor is defined as

$$q(\psi) = \oint \frac{B_z}{B_p} \frac{dl}{2\pi r},$$

(13)

where ψ is the magnetic flux. Figure 5 shows the profile of the safety factor q for the three geometries as a function of the normalized flux, defined as $(\psi - \psi_0)/(\psi_{sep} - \psi_0)$, where ψ_0 is the minimum magnetic flux in the core plasma and ψ_{sep} is the magnetic flux at the separatrix.

The value of q at the center increases considerably with the increase of the ellipticity. In Fig 6 axial magnetic fluctuations are shown in various poloidal cross-sections. The fluctuations of the axial magnetic field are obtained by showing the magnetic field without the axially invariant ($k_z = 0$) magnetic contribution. Only in a few sections a clear poloidal mode structure is observed. These graphs, combined with the spectra shown in Figure 4 give a hint about the possible instabilities underlying the dynamics. Tearing modes are known to appear on places in the plasma where the ratio $m/n = q$ is close to a rational number. For the circular geometry, where an $n = 7$ magnetic toroidal mode is dominant, in one of the cross-sections a clear $m = 1$ poloidal structure can be identified. The value $q = m/n = 1/7$ is not attained in the plasma, but this value is approached in the center of the domain (see Figure 5(d)). The triggered instability could possibly be associated with an ideal kink mode. For the elliptical cylinder with $a = 1.2$, a hint of $m = 1$ and $m = 2$ structures is visible in the cross-sections taken at instant $t = 9.8 \times 10^3 \tau_A$, where the $n = 14$ magnetic mode is dominant. The same analysis at different instants where no magnetic
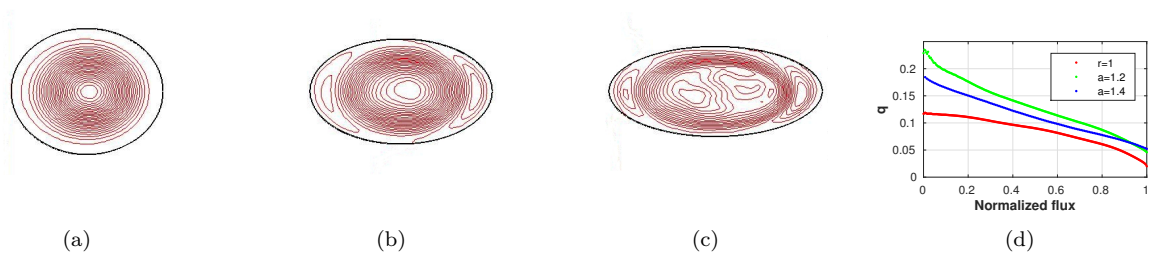
FIG. 5: *Profile of the safety factor q function of the normalized flux, for the three geometries at* $t = 9.8 \times 10^3 \tau_A$. *Flux surfaces for the three geometries.*

mode n dominates, shows the persistance of the poloidal mode $m = 2$. Thus, both rational surfaces $q = 1/14$ and $q = 2/14$ are within the plasma, so that in this case external tearing modes are a candidate to explain the underlying dynamics, even though modes near the axis are generally observed to be more unstable. The conclusion from these observations is that shaping significantly influences the velocity and magnetic fields, both qualitatively and quantitatively.
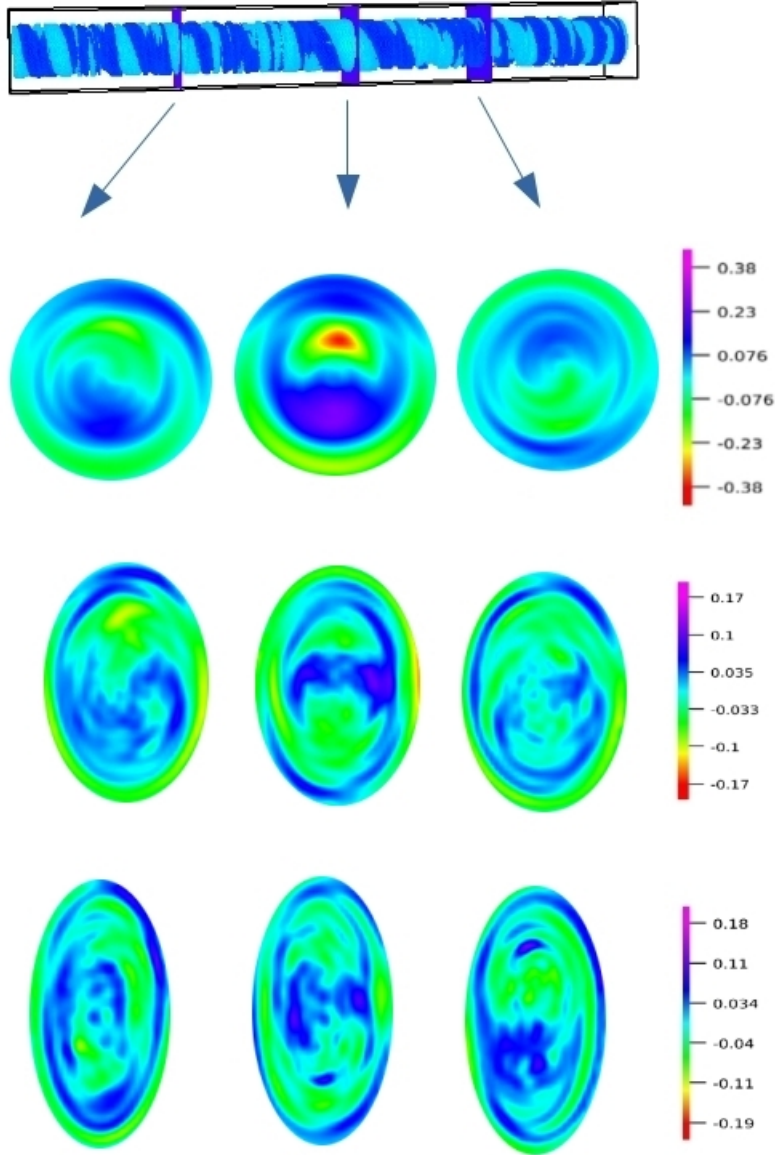
FIG. 6: Poloidal cross-sections of the cylinder for circular (top) and the two elliptical (center, bottom) geometries, illustrating the axial magnetic fluctuations at $t = 9.8.10^3 \tau_A$.

3.3 Turbulent diffusion

In order to assess the influence of the velocity field on the confinement, we have compared the radial diffusion of a passive scalar in the different geometries. By fixing the rate of injection at the same value for all three geometries, the confinement can be evaluated by the mean scalar profile which establishes in the statistically stationary state. A difficulty in the comparison is here the fact that for the elliptical cross section, the scalar profile depends on the angle, and that in any case the maximum scalar does not need to be exactly in the center. What is important for confinement, is the maximum temperature, not necessarily its spatial location. In order to overcome all these difficulties, we define a sorted scalar profile, by sorting all scalar values in the plasma from high to low. By properly normalizing the x-axis, we
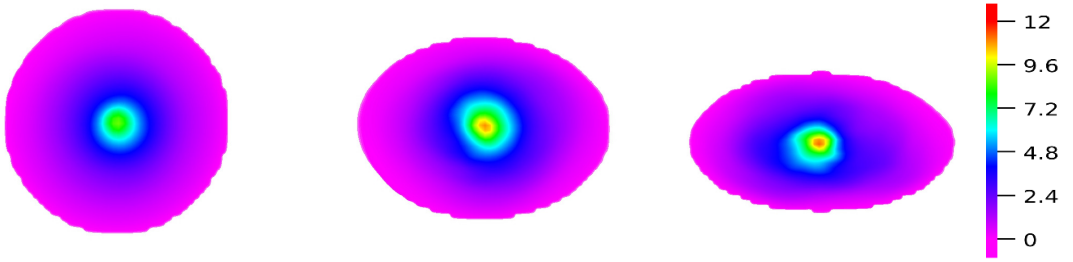
FIG. 7: Cross-section of the scalar field for different shapes, for $S \sim 2.10^4$ and $L_z/2\pi b = 4$.

convert this sorted dataset into an effective scalar profile, corresponding to a circular, perfectly centered, axisymmetric scalar distribution. **This procedure is somewhat similar to the introduction of a magnetic flux function in tokamak studies. However, here the ordering of the spatial points is carried out as a function of isothermal contours. This type of sorting of temperature profiles is common in studies of stratified turbulence [31].**

In practice, these profiles are obtained by sorting the different points in the fluid domain of each plane orthogonal to the z-axis, in decreasing order of scalar value, then averaging over the volume. All geometries have the same number of points in the fluid domain because of the equal cross-sections. The sorted profiles are shown in Figure 8 left. The x-axis is now a function of the generalized radius $\tilde{r}$. **This generalized radius is defined by**

$$\tilde{r} = \sqrt{\frac{n}{N}} r_0 \tag{14}$$

where N is the total number of measurement points, n the n-th point of the sorted values and r_0 the reference radius, which equals 1 in our case. For non-axisymmetric profiles and cross-sections this representation will allow a direct comparison between the different scalar distributions.

Figure 7 and 8 show that the elliptical cases have the highest scalar value in the center of the plasma. The turbulent diffusion associated to the chaotic-turbulent motion can be directly evaluated from the average scalar profile by introducing an effective diffusivity D_T defined by,

$$D_T = \frac{G}{\tilde{r}\frac{\partial \langle T \rangle}{\partial \tilde{r}}} \qquad \forall \, \tilde{r} > r^* \tag{15}$$

where G is the total injected heat computed from the scalar source term,

$$G = -\iint_0^{r^*} f_T r d\theta dr, \qquad \text{with} \quad r^* = 0.1. \tag{16}$$

A peak in the diffusivity profile in the near-wall region $0.8 < \tilde{r} < 1$ is observed, which could possibly be associated with an enhanced level of turbulence, generated in the shear-layer between the helical structure and the wall.

A further, more detailed characterization of the transport, probing the stochasticity of the flow, using for instance Poincaré maps, would be an interesting perspective. Also, considering directly the Ohmic heating as a source term, would be an elegant way to investigate the temperature diffusion in a self-consistent manner.

4 On the choice of different characteristic scales

Different physical systems can only be meaningfully compared if the dimensionless parameters of the system are evaluated. These dimensionless numbers appear in general when the evolution equations of the system are non-dimensionalized by appropriate length, time, magnetic and other relevant scales.
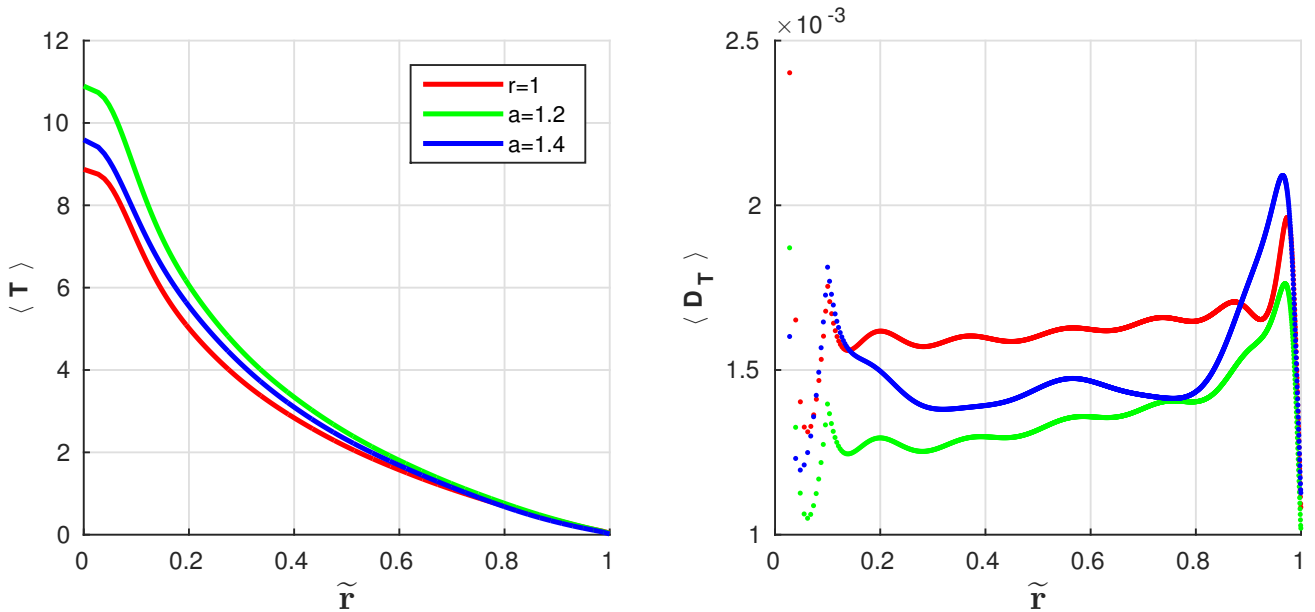
FIG. 8: *Mean scalar profiles as a function of the generalized radial coordinate $\tilde{r}$ (left). Effective diffusivity profile normalized by the cross-sectional surface. Both profiles are time-averaged over $3 \times 10^3 \tau_A$ (right).*

Hereby appear, for the case of MHD, dimensionless quantities like the Hartmann and Lundquist number. For example, the Hartmann number defined as,

$$Ha = \frac{C_A \mathcal{L}}{\sqrt{\eta \nu}}, \tag{17}$$

where η is the magnetic resistivity, $\mathcal{L}$ is a characteristic length scale and C_A the Alfvén velocity, plays a major role in describing laminar MHD dynamics [32–34] and the transition from multi-helical states to single-helical states [22]. On the other hand, the Lundquist number S is generally used in the fusion community to describe the plasma dynamics in the turbulent regime. For our case, where $\eta = \nu$, those two numbers have equal values, $Ha = S$. An important question is now how to define the length scale $\mathcal{L}$.

In the case of a circular cross-section, the most logical choice of a reference length scale is the radius of the cylinder. Deforming the cross-section breaks the symmetry of the problem, and the radius is not longer uniquely defined by a simple number. A rather logical choice of the reference length is now $\mathcal{L} = \sqrt{ab}$, but this choice is not free from some arbitrariness. Another relevant length scale could be b, the minor axis, since this length scale is the smallest distance from the center to the wall, and as such it could pilot the confinement quality of the plasma. The choice of these two different typical length scales leads, for a given toroidal magnetic field and Lundquist number, to distinct values of the magnetic diffusivity. We have therefore considered two different choices for $\mathcal{L}$ and evaluated their impact onto the dynamics. The parameters of different cases are summarized in table I.

First, the evolution of the kinetic energy and average scalar value for cases 1 and 2, having the same characteristic magnetic scale and different lengthscales, are considered and presented in Figure 9. For $\mathcal{L} = b$, the kinetic energy fluctuates around the same value for the three geometries. For this case, which we considered in the previous sections, the value of the scalar in the elliptical geometries is larger than that observed in the circular one. **On the other hand, for $\mathcal{L} = \sqrt{ab}$, the kinetic energy fluctuates around the same value in the elliptical cases, and it is slightly larger than the one of the circular case. While the evolution of kinetic energy is close in cases 1 and 2, the evolution of the scalar shows a drastic change. Furthermore, the mean of the scalar value for the**

	r	a	b	C_A	$\mathcal{L}$	λ
	1	-	-	$\overline{B_p} = 1.4$	r	1.4×10^{-4}
Case 1	-	1.2	0.83	$\overline{B_p} = 1.36$	b	1.1×10^{-4}
	-	1.4	0.71	$\overline{B_p} = 1.26$	b	9×10^{-5}
	1	-	-	$\overline{B_p} = 1.4$	r	1.4×10^{-4}
Case 2	-	1.2	0.83	$\overline{B_p} = 1.36$	$\sqrt{ab}$	1.35×10^{-4}
	-	1.4	0.71	$\overline{B_p} = 1.26$	$\sqrt{ab}$	1.25×10^{-4}

TABLE I: Parameters for case 1 where $\mathcal{L} = b$ and case 2 where $\mathcal{L} = \sqrt{ab}$, for the three geometries.

elliptical cases decreases, to reach the same value of the circular case for $a = 1.2$, and a smaller value for $a = 1.4$.

5   Conclusion

Direct numerical simulations of viscoresistive MHD show that in periodic cylindrical geometry in the RFP regime, the shape of the cross-section significantly changes the nonlinear dynamics. Moreover, different helical states can be observed and different energetic modes are excited in different geometries. Modifying the elliptical elongation leads to different modal behaviors. **We quantified the impact on the confinement properties by considering the radial advection of a passive scalar, injected in the center of the domain**. Indeed, the evaluation of the eddy-diffusivity shows a clear enhancement of the confinement quality for elliptic cross-sections.

The physical reason why elongation could enhance confinement deserves certainly further investigation.

One possibility is that changing the geometry, for given current and toroidal magnetic field, will lead to a self-organized state with a different level of magnetic fluctuations. We have carried out supplementary computations in which we increased the axial magnetic field
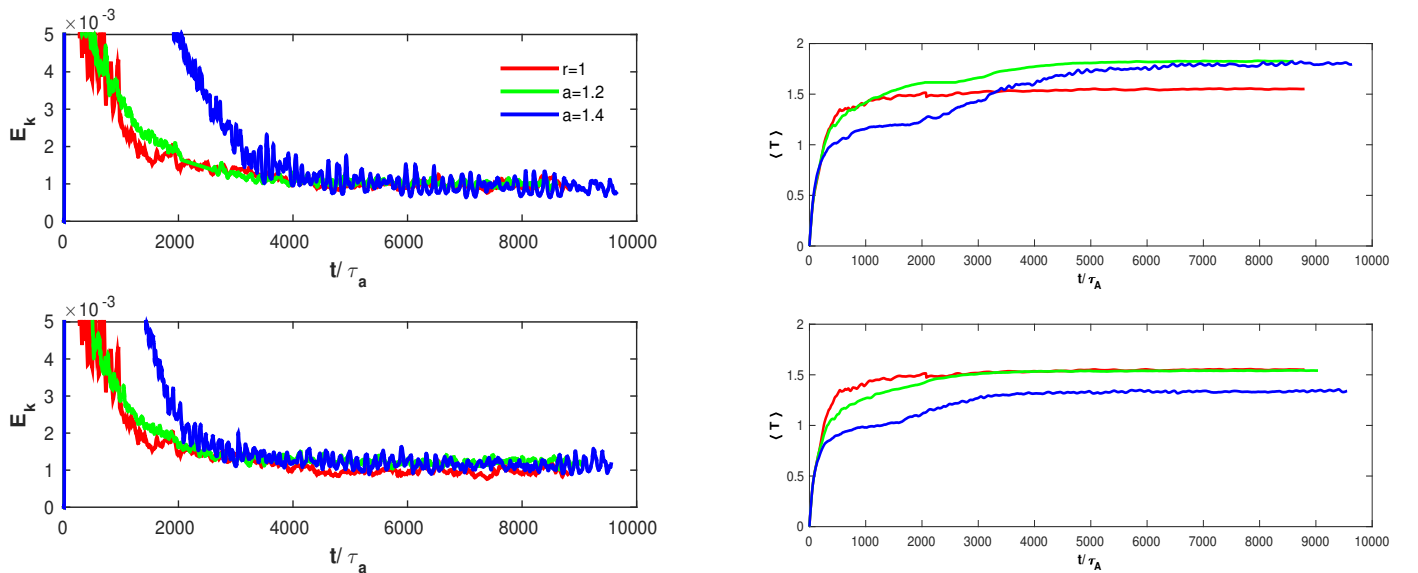

FIG. 9: Evolution in time of the kinetic energy E_k (left), and the mean of the scalar value $\langle T \rangle$ (right), respectively from top to bottom for cases 1 and 2.

for the circular geometry, thereby lowering the initial pinch by a factor 1.75. **The increased stability in this case led to a lower level of magnetic fluctuations. However, even in this case in which the turbulent magnetic activity was of the level of the elliptic case (with $a = 1.2$) the safety factor remained roughly unchanged, and so did the diffusion. It seems thus that a change in the geometry affects the self-organized state with respect to the safety factor and diffusion, and that this result persists even when the initial pinch ratio is significantly changed.**

Another possibility is that elongation leads to symmetry breaking of the poloidal flow. Indeed in 2D turbulence, changing the flow-geometry from circular to elliptical, leads to the generation of angular momentum [35]. This effect was shown to persist in 2D MHD turbulence [36] and its investigation is considered an interesting perspective, since large scale poloidal motion could enhance radial transport barriers. **A preliminary investigation of this effect is shown in Figure 10 where for a given time-instant the angular momentum associated with the poloidal flow is computed for each cross-section. Even though the total volume averaged angular momentum might be small, it is shown that for the case of the circular geometry, locally large values of the poloidal angular momentum exist.**

The most important message of this work is perhaps not the knowledge of a certain value of the elongation, most efficient to obtain an optimal confinement, but the mere fact that elongation can change the confinement of RFPs. We would therefore encourage experimentalists to consider the poloidal shape of the confining magnetic field as an important control parameter for RFP design and operation. If an experiment allows for a simple modification of the plasma shape, it might give more freedom to obtain a competitive fusion plasma.

Acknowledgments
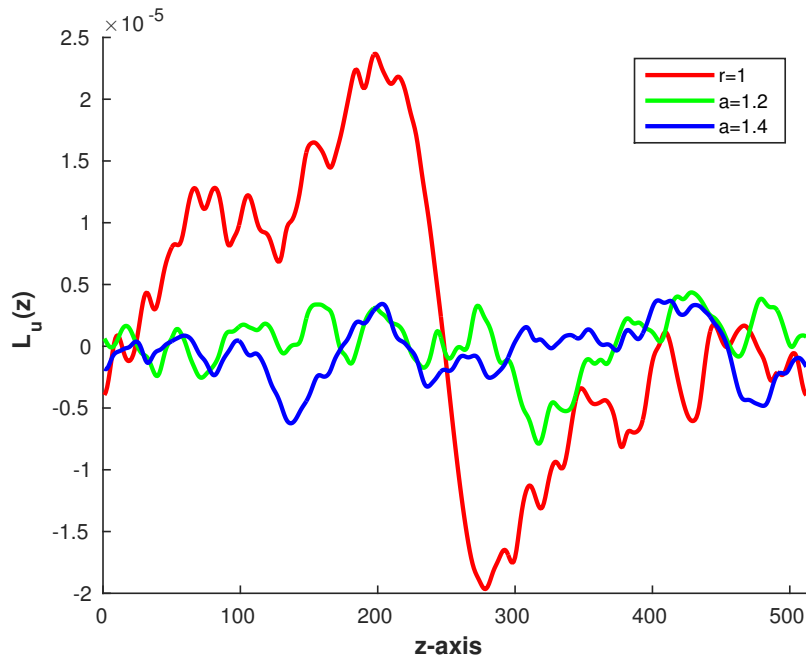
FIG. 10: *z-dependence of the instantaneous poloidal angular momentum for the three geometries at* $t = 11 \times 10^3 \tau_A$.

References

[1] D. Biskamp. *Nonlinear magnetohydrodynamics.* Cambridge University Press, 1993.

[2] D. F. Escande, P. Martin, S. Ortolani, A. Buffa, P. Franz, L. Marrelli, E. Martines, G. Spizzo, S. Cappello, A. Murari, R. Pasqualotto, and P. Zanca. Quasi-single-helicity reversed-field-pinch plasmas. *Phys. Rev. Lett.*, 85:1662, (2000).

[3] P. Martin *et al.* Quasi-single helicity states in the reversed field pinch: Beyond the standard paradigm. *Phys. Plasmas*, 24, (2000).

[4] P. Martin *et al.* Overview of quasi-single helicity experiments in reversed field pinches. *Nucl. Fusion*, 43, (2003).

[5] L. Frassineti, I. Predebon, H. Koguchi, Y. Yagi, Y. Hirano, H. Sakakita, G. Spizzo, and R.B. White. Improved particle confinement in transition from multiple-helicity to quasi-single-helicity regimes of a reversed-field pinch. *Phys. Rev. Lett.*, 97, (2006).

[6] D. Terranova, A. Alfier, F. Bonomo, P. Franz, P. Innocente, and R. Pasqualotto. Enhanced confinement and quasi-single-helicity regimes induced by poloidal current drive. *Phys. Rev. Lett.*, 99, (2007).

[7] M. D. Wyman *et al.* Plasma behaviour at high β and high density in the Madison Symmetric Torus RFP. *Phys. Plasmas*, 15, (2008).

[8] P. Piovesan *et al.* Magnetic order and confinement improvement in high-current regimes of RFX-mod with MHD feedback control. *Nucl. Fusion*, 49, (2009).

[9] P. Piovesan *et al.* Influence of external 3D magnetic fields on helical equilibrium and plasma flow in RFX-mod. *Plasma Phys. Control. Fusion*, 53, (2011).

[10] P. Piovesan *et al.* RFX-mod: A multi-configuration fusion facility for three-dimensional physics studies. *Phys. Plasmas*, 20, (2013).

[11] R. Lorenzini *et al.* Self-organized helical equilibria as a new paradigm for ohmically heated fusion plasmas. *Nature Phys.*, 5, (2009).

[12] D Bonfiglio, M Veranda, S Cappello, DF Escande, and L Chacón. Experimental-like helical self-organization in reversed-field pinch modeling. *Physical review letters*, 111(8):085002, 2013.

[13] F. Troyon, R. Gruber, H. Saurenmann, S. Semenzato, and S. Succi. MHD-limits to plasma confinement. *Plasma Phys. Control. Fusion*, 26, (1984).

[14] A.F. Almagri, S. Assadi, R.N. Dexter, S.C. Prager, J.S. Sarff, and J.C. Sprott. *Nucl. Fusion*, 27, (1987).

[15] A.A.M. Oomens, H.S. Lassing, and A.F.G. Van Der Meer. Reversed Field Pinch discharges with elongated minor cross-section. *Rijnhuizen report 90-197*, (1990).

[16] R. Paccagnella, A. Bondeson, and H. Lütjens. Ideal toroidal stability beta limits and shaping effect for reversed field pinch configurations. *Nucl. Fusion*, 31(10), (1991).

[17] S.C. Guo, X.Y. Xu, Z.R. Wang, and Y.Q. Liu. Does shaping bring an advantage for reversed field pinch plasmas? *Nucl. Fusion*, 53, (2013).

[18] J. A. Morales. *Confined magnetohydrodynamics applied to magnetic fusion plasmas.* PhD thesis, Ecole Centrale de Lyon, (2013).

[19] J. A. Morales, W. J.T. Bos, K. Schneider, and D. Montgomery. On the effect of toroidicity on reversed field pinch dynamics. *Plasma Phys. Control. Fusion*, 56, (2014).

[20] S. Futatani, J. A. Morales, and W. J.T. Bos. Dynamic equilibria and magnetohydrodynamic instabilities in toroidal plasmas with non-uniform transport coefficients. *Phys. Plasmas*, 22, (2015).

[21] S Cappello and D Biskamp. Reconnection processes and scaling laws in reversed field pinch magnetohydrodynamics. *Nucl. Fusion*, 36:571, 1996.

[22] S. Cappello and D. F. Escande. Bifurcation in viscoresistive MHD: The hartmann number and the reversed field pinch. *Phys. Rev. Lett.*, 85, (2000).

[23] John M Finn, Rick Nebel, and Charles Bathke. Single and multiple helicity ohmic states in reversed-field pinches. *Physics of Fluids B: Plasma Physics*, 4(5):1262–1279, 1992.

[24] D Bonfiglio, S Cappello, and DF Escande. Impact of a uniform plasma resistivity in mhd modelling of helical solutions for the reversed field pinch dynamo. *arXiv preprint arXiv:1603.03563*, 2016.

[25] C. Canuto, M. Hussaini, A. Quarteroni, and T. Zang. *Spectral Methods in Fluid Dynamics.* Springer, 1987.

[26] J. A. Morales, M. Leroy, W. J.T. Bos, and K. Schneider. Simulation of confined magnetohydrodynamic flows with Dirichlet boundary conditions using a pseudo-spectral method with volume penalization. *J. Comp. Phys.*, 274, (2014).

[27] J.B. Taylor. Relaxation of toroidal plasma and generation of reverse magnetic fields. *Phys. Rev. Lett.*, 33, (1974).

[28] A. Reiman. Minimum energy state of a toroidal discharge. *Phys. Fluids*, 23, (1980).

[29] A. Reiman. Taylor relaxation in a torus of arbitrary aspect ratio and cross section. *Phys. Fluids*, 24, (1981).

[30] J. B. Taylor. Relaxation and magnetic reconnection in plasmas. *Rev. Mod. Phys.*, 58, (1986).

[31] S.A. Thorpe. Turbulence and mixing in a Scottish loch. *Phil. Trans. Roy. Soc. London A*, 286:125–181, 1977.

[32] D. Montgomery. Magnetohydrodynamic stability thresholds as a function of Hartmann number and pinch ratio. *Plasma Phys. Control. Fusion*, 34, (1992).

[33] D. Montgomery. Hartmann, Lundquist, and Reynolds: the role of dimensionless numbers in nonlinear magnetofluid behavior. *Plasma Phys. Control. Fusion*, 35, (1993).

[34] X. Shan and D. Montgomery. On the role of the Hartmann number in magnetohydrodynamic activity. *Plasma Phys. Control. Fusion*, 35, (1993).

[35] G. H. Keetels, H. J. H. Clercx, and G. J. F. van Heijst. Spontaneous angular momentum generation of two-dimensional fluid flow in an elliptic geometry. *Phys. Rev. E*, 78, (2008).

[36] W. J. T. Bos, S. Neffaa, and K. Schneider. Self-organization and symmetry-breaking in two-dimensional plasma turbulence. *Phys. Plasmas*, 17, (2010).